Electronic Supplementary Information

Mesoporous Cerium Oxide-Coated Upconversion Nanoparticles for Tumor-Responsive Chemo-Photodynamic Therapy and Bioimaging

Tao Jia,‡[a] Jiating Xu,‡[a] Shuming Dong,[a] Fei He,*[a] Chongna Zhong,[a] Guixin Yang,[a] Huiting Bi,[a] Mengshu Xu,[a] Yingkui Hu,[a] Dan Yang,[a] Piaoping Yang,*[a] and Jun Lin*[b]

[a] Key Laboratory of Superlight Materials and Surface Technology, Ministry of Education, College of Material Sciences and Chemical Engineering, Harbin Engineering University, Harbin, 150001, P. R. China

[b] State Key Laboratory of Rare Earth Resource Utilization, Changchun Institute of Applied Chemistry, Chinese Academy of Sciences, Changchun 130021, P. R. China

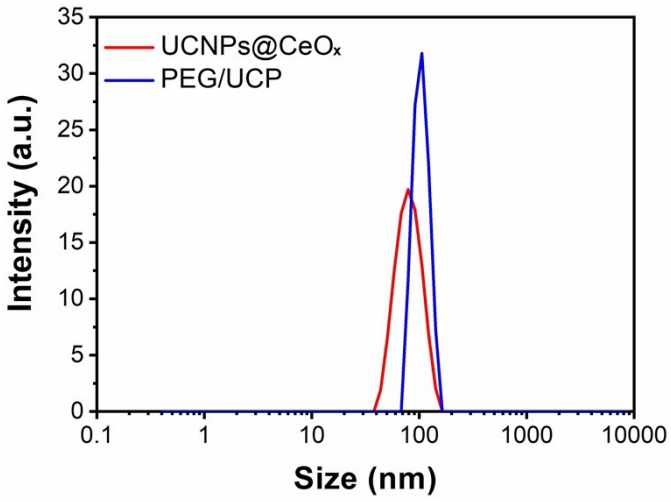

Fig. S1 The particle size distributions of UCNPs@$mSiO_2$, UCNPs@CeO_x and PEG/UCP in water measured by dynamic light scattering (DLS).

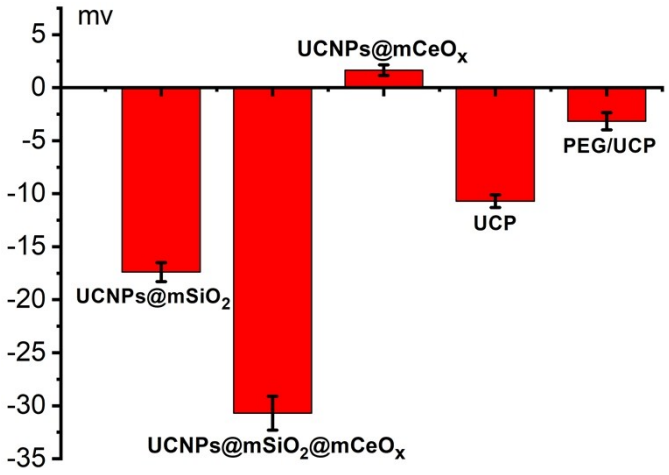

Fig. S2 Zeta potentials of UCNPs@mSiO$_2$, UCNPs@mSiO$_2$@mCeO$_x$, UCNPs@mCeO$_x$, UCP and PEG/UCP.

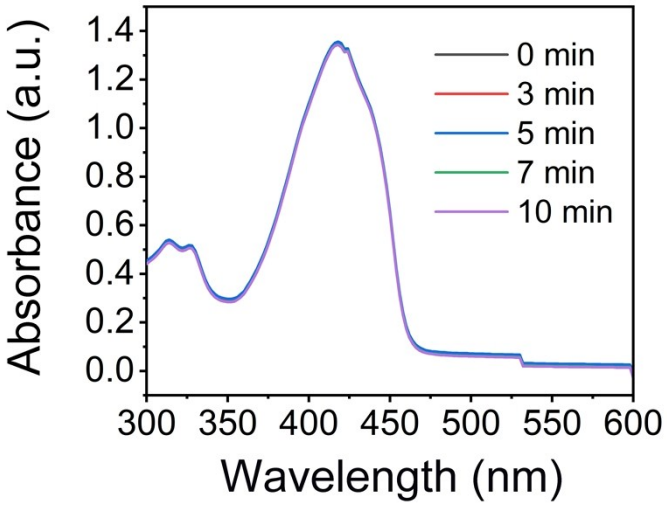

Fig. S3 The absorbance of DPBF solutions with UCNPs@mCeO$_x$ at different time periods.

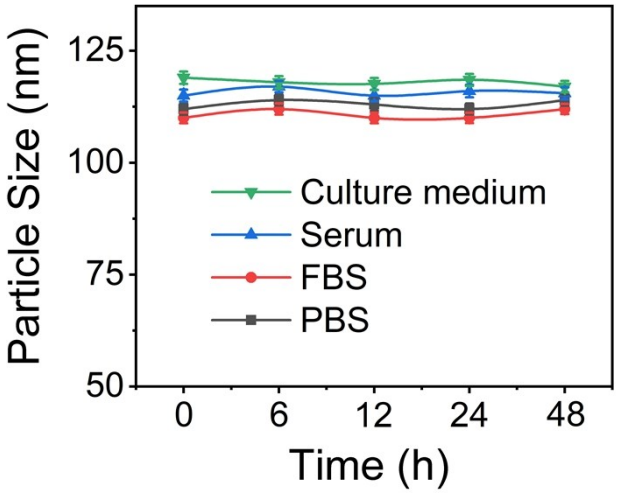

Fig. S4 The particle size distributions of the supernatant obtained from the PEG/UCP solutions in PBS (pH 7.4) and FBS, serum and culture medium after two days standing.

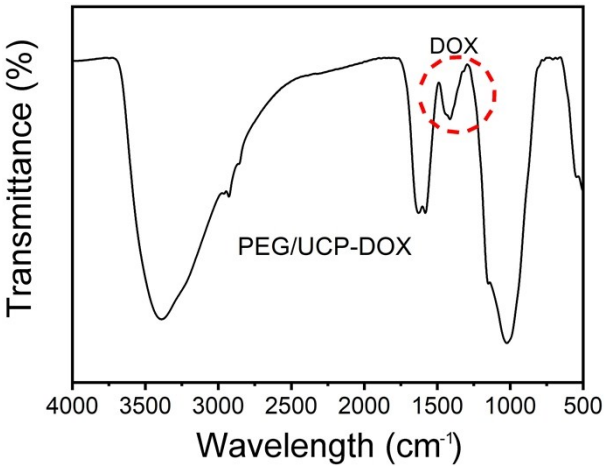

Fig. S5 FT-IR spectrum of PEG/UCP-DOX.

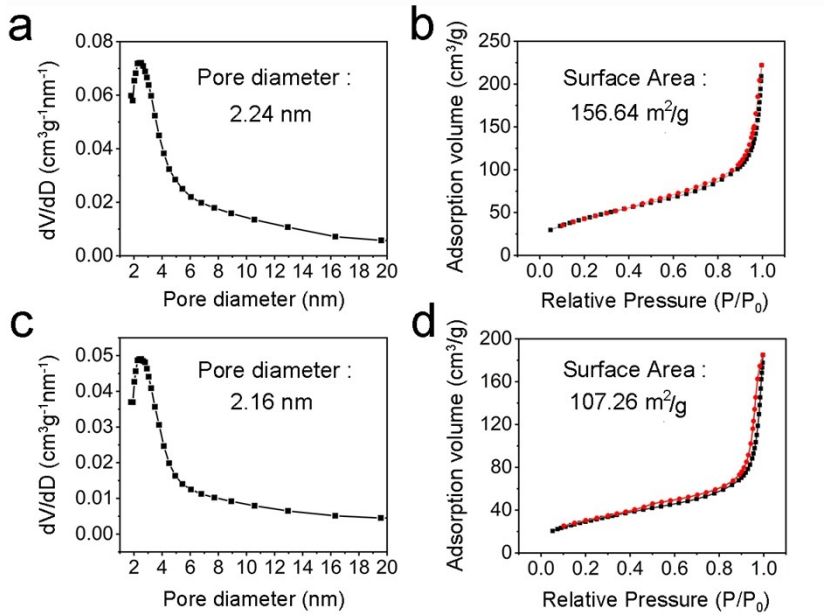

Fig. S6 N_2 adsorption/desorption isotherms and corresponding pore size distribution curves of PEG/UCP (a, b) and PEG/UCP-DOX samples (c, d).

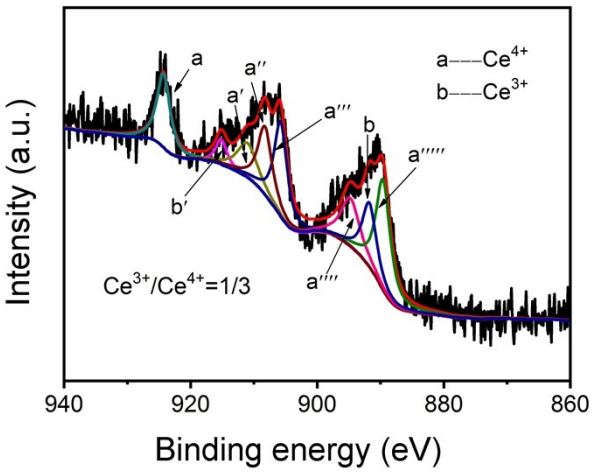

Fig. S7 XPS analysis to show the chemical valence of cerium on the surface of UCNPs@mCeO$_x$.

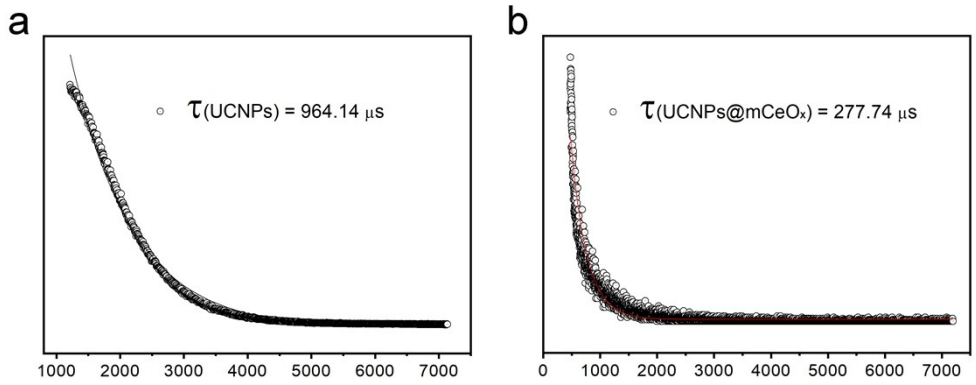

Fig. S8 Decay curves of Tm^{3+} at 475 nm in UCNPs@$mCeO_x$ and UCNPs samples upon 980 nm laser excitation.

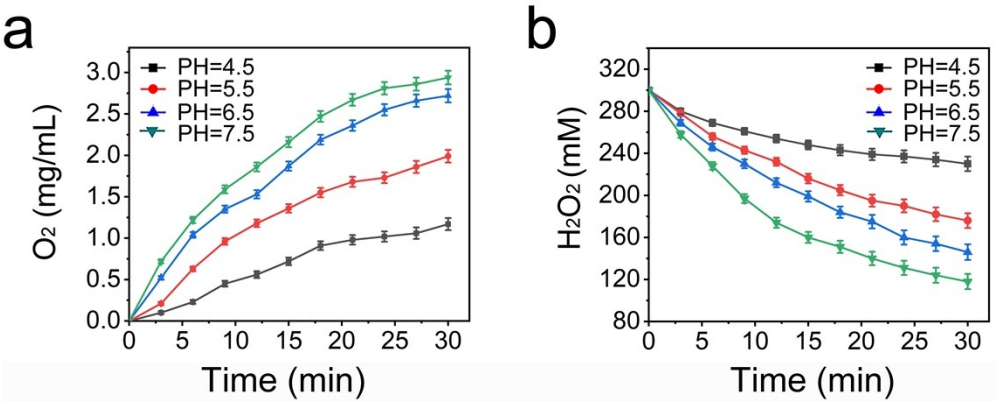

Fig. S9 O_2 production rate (a) and H_2O_2 decomposition rate (b) catalyzed by UCNPs@mCeO$_x$ at different time in absence of NIR light irradiation.

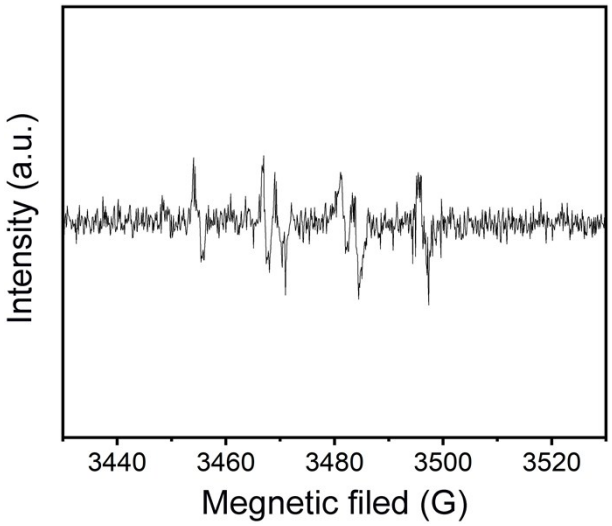

Fig. S10 ESR spectrum for detection of superoxide anion *versus* magnetic field.

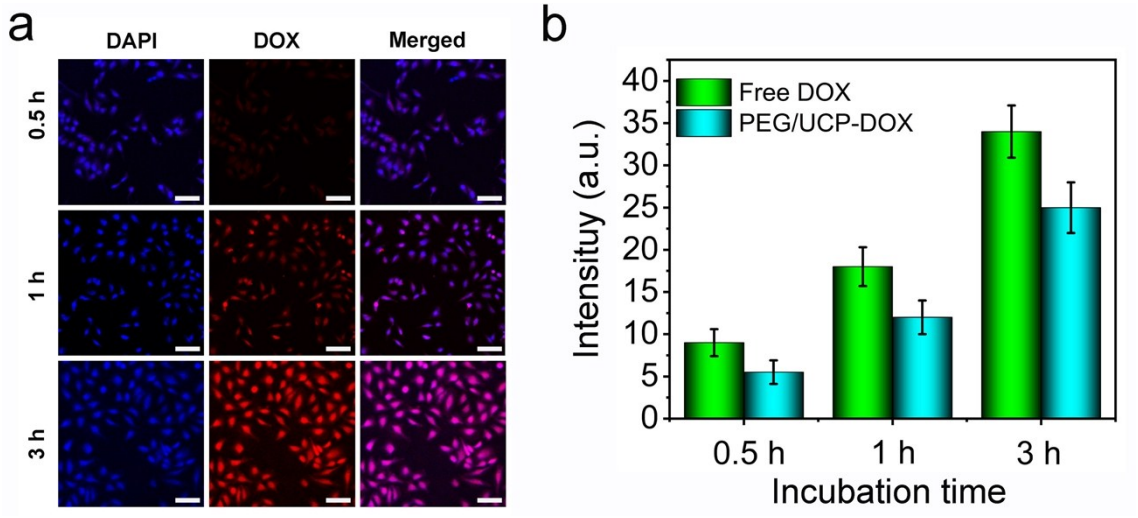

Fig. S11 UCLM images of HeLa cells incubated with free DOX at 37 °C for 0.5, 1, and 3 h. Fluorescence intensity of HeLa after incubation with free DOX and PEG/UCP-DOX for 0.5 h, 1 h and 3 h via image-pro plus (b). Scale bar: 50 μm.

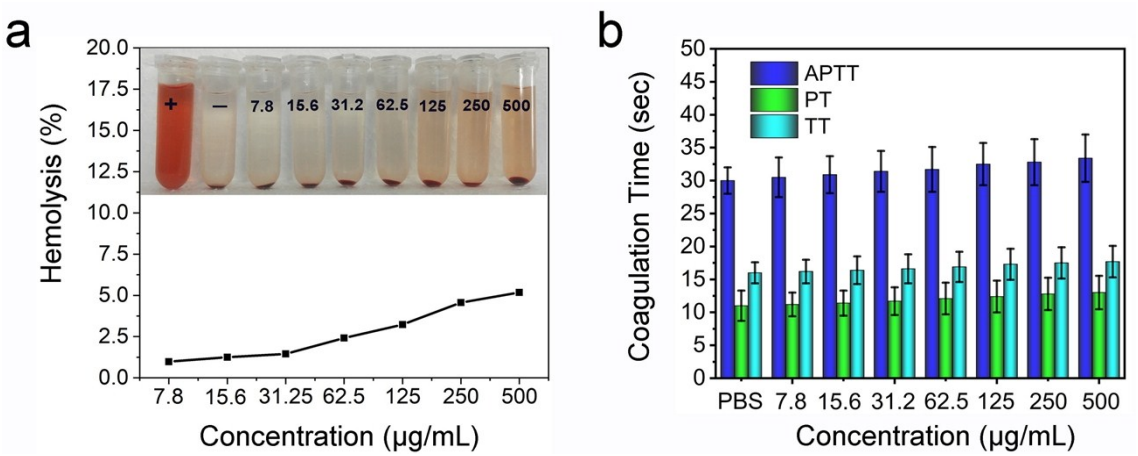

Fig. S12 Hemolysis assay for PEG/UCP (inset: photographic images for direct observation of hemolysis by PEG/UCP using PBS as a negative control and water as a positive control (left two tubes), and PEG/UCP suspensions with different concentrations) (a) and the coagulation time of PBS (as control) and different concertrations of samples (PEG/UCP) were evaluated by activated partial thromboplastin time (APTT), prothrombin time (PT) and thrombin time (TT).

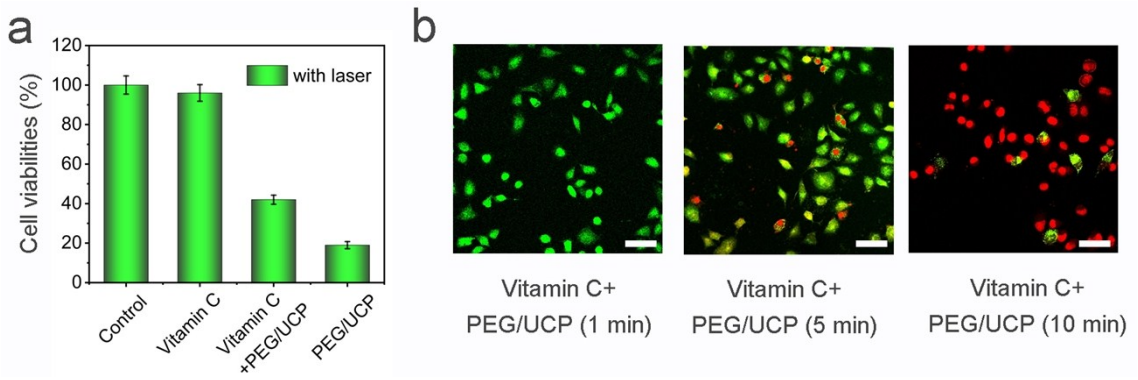

Fig. S13 Cell cytotoxicity of control, different inhibitors with PEG/UCP incubated with HeLa cell by the MTT assay (a), CLSM image of HeLa cancer cells incubated with different irradiation time (b). All the cells were dyed with Calcein AM and PI images share the same scale bar of 50 μm.

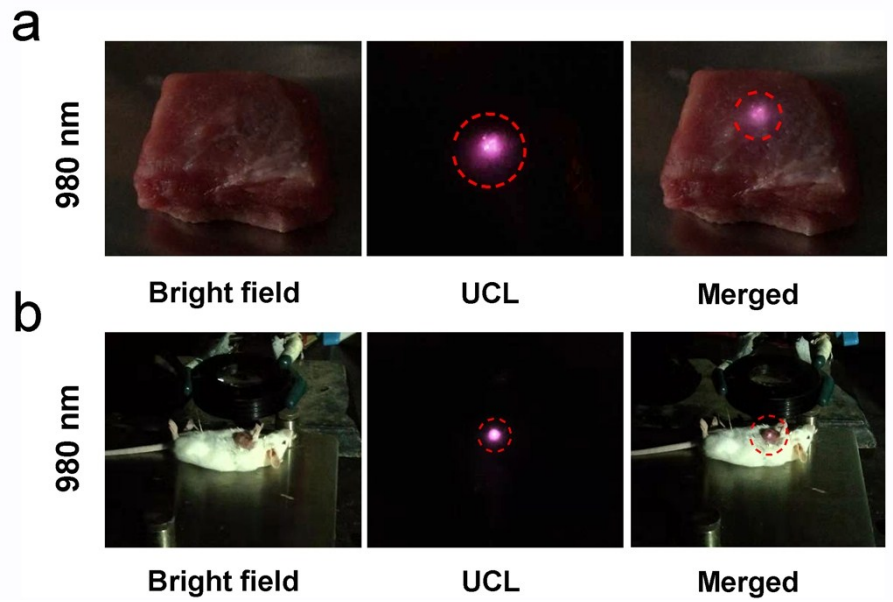

Fig S14 Bright field, UCL and merged images of pork muscle tissues injected with PEG/UCP at depth of ~8 mm (a) and a mouse injected with PEG/UCP (b) upon 980 nm laser irradiation. The laser pump powers are 0.72 W cm^{-2}.

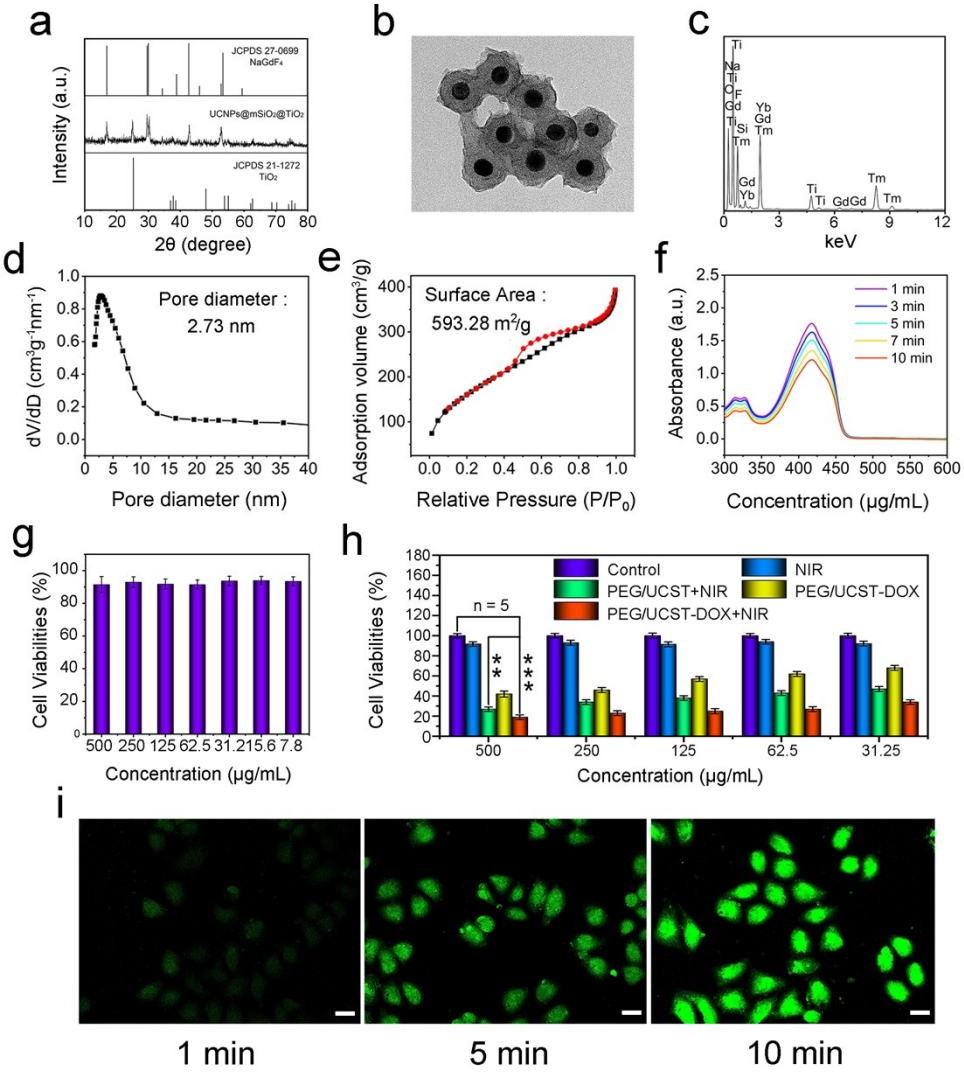

Fig. S15 XRD patterns of UCNPs and UCNPs@mSiO$_2$@mTiO$_2$ (the standard pattern of β-NaGdF$_4$ and TiO$_2$ are supplied for comparison) (a), TEM image of UCNPs@mSiO$_2$@mTiO$_2$ (b), EDS spectrum of UCNPs@mSiO$_2$@mTiO$_2$ (c), the pore-size distribution (d) and N$_2$ absorption/desorption isotherm (e) of UCNPs@mSiO$_2$@TiO$_2$. The absorbance of DPBF solutions with UCNPs@mSiO$_2$@TiO$_2$ at different time periods under 980 nm laser radiation (0.72 W cm^{-2}) (f). Cell viabilities of L929 fibroblast cells with incubation of different PEG/UCST (g). Cell viability *versus* incubated particle concentration (7.8, 15.6, 31.2, 125, 250, and 500 μg mL^{-1}) for HeLa cells under different conditions (Control, NIR, UCNPs@mSiO$_2$@mTiO$_2$, PEG/UCST-DOX, and PEG/UCST-DOX+ NIR) Mean ± s. d, n = 5. P values were calculated by Tukey's post-test (***$p < 0.001$) (h), and the CLSM images of HeLa cells with oxidized DCF fluorescence at different illumination times. Scale bar: 50 μm (i).

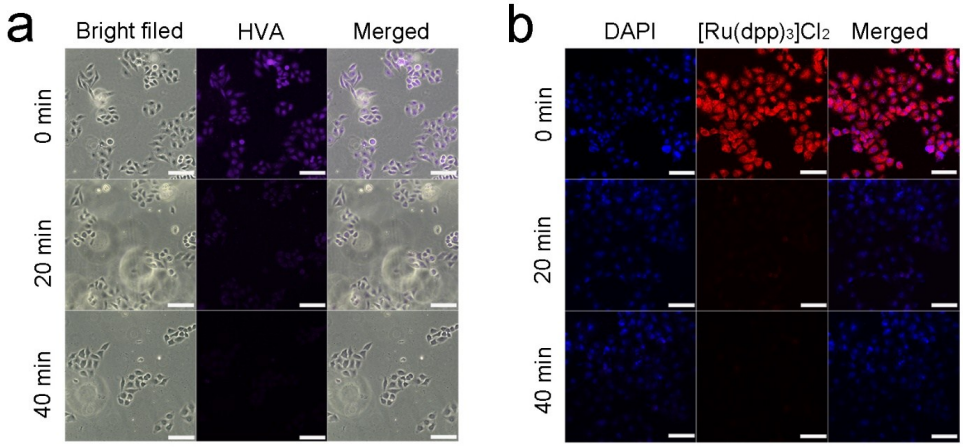

Fig. S16 The CLSM images of HeLa cells at different 980 nm laser irradiation time, the cells were incubated with PEG/UCP and incubated with HVA as the H_2O_2 probes (a) and stained with Dapi and $[Ru(dpp)_3]Cl_2$ as the nucleus and dissolved O_2 probes, respectively (b). Scale bars stand for 50 μm.

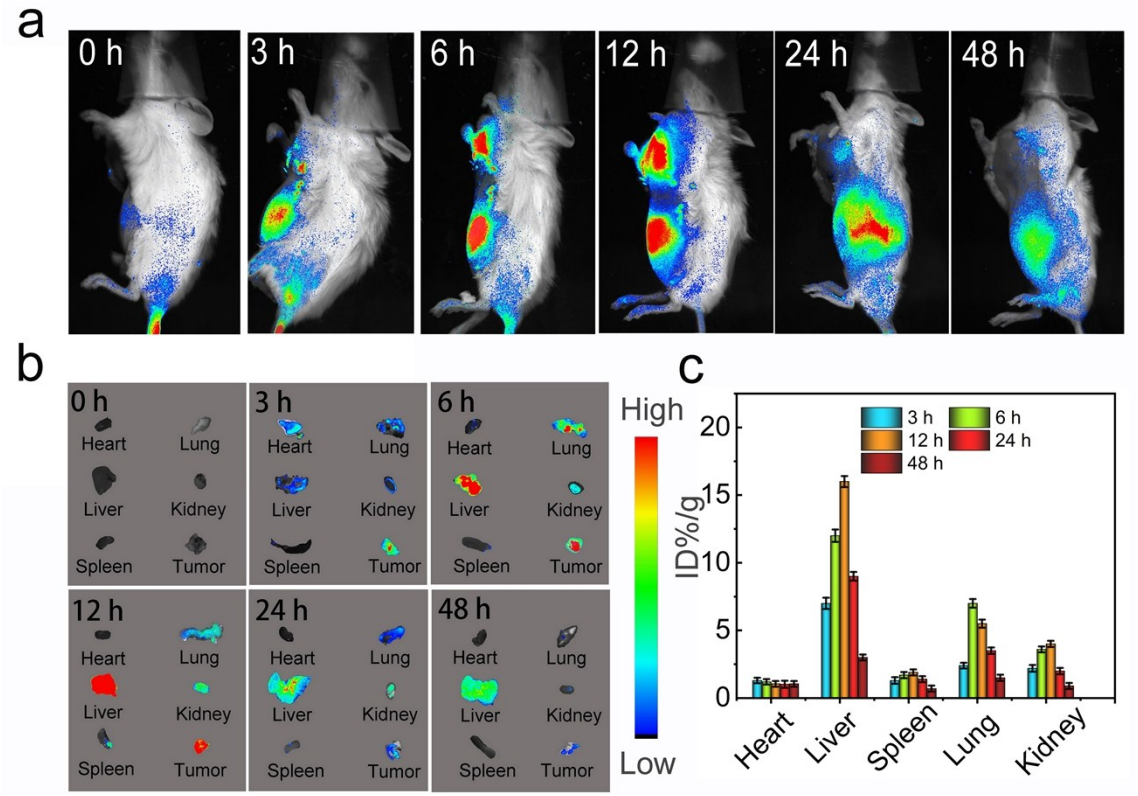

Fig. S17 *In vivo* FL images of U14-tumor-bearing nude mice taken after *i.v.* injection of the PEG/UCP assembly (a). Ex *vivo* FL images of major organs and tumors at different time intervals postinjection with the PEG/UCP assembly (b). Time-dependent concentrations of Ce in the major organs as measured by ICP-MS (c).

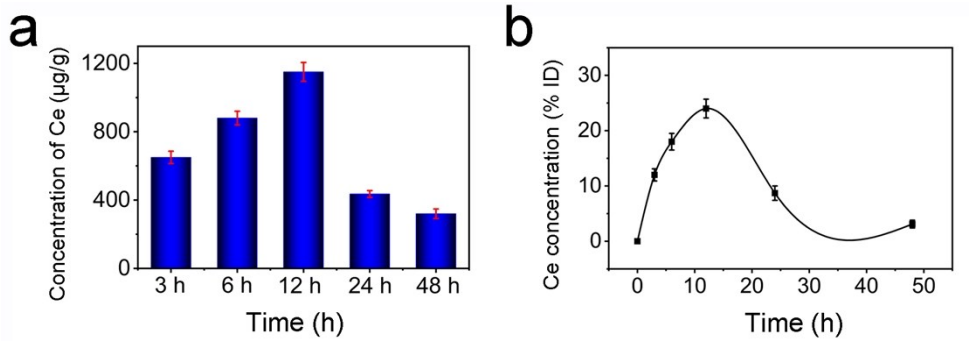

Fig. S18 The biodistribution of Ce in tumor of mice after injection of PEG/UCP at different time points (a). Accumulation effect of the PEG/UCP nanoparticles in tumor site (b). Error bars indicate standard deviations, n = 3.

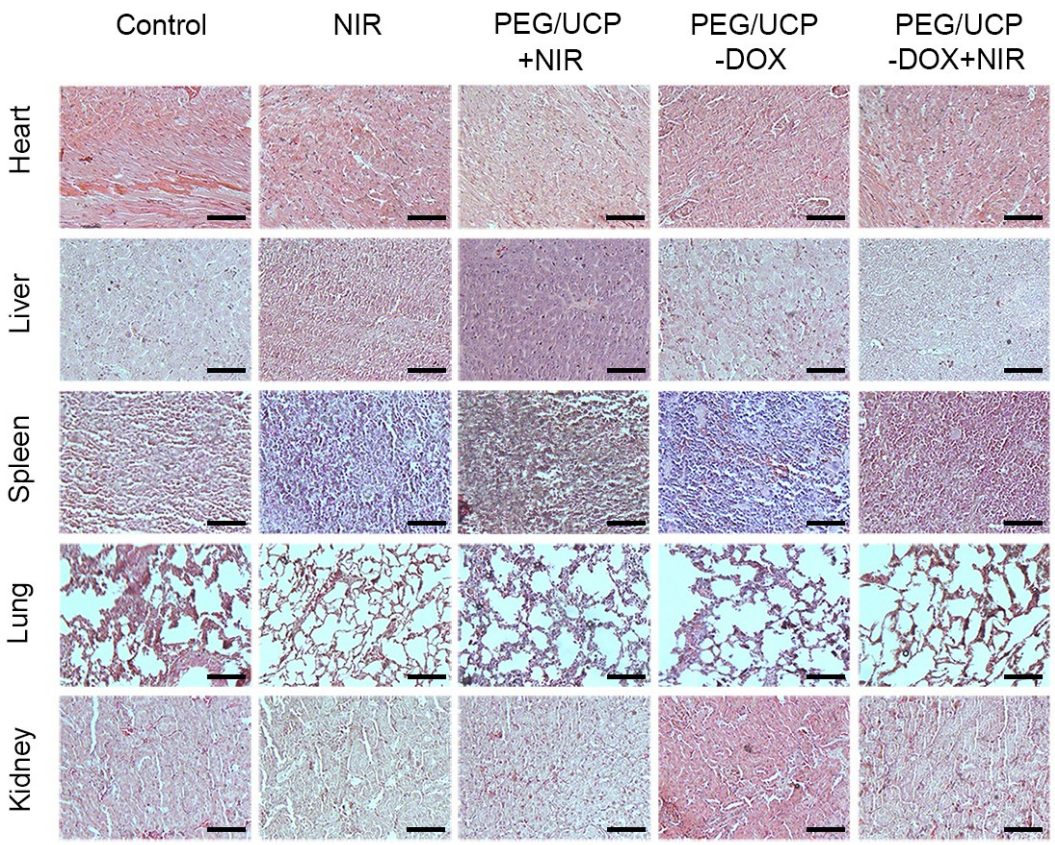

Fig. S19 H&E stained images of heart, liver, spleen, lung, and kidney collected from different groups after treatment for 2 weeks. Scale bar: 50 μm.

Table S1. Blood biochemistry and hematology data of female mice

Project Name	Treatment Group Mean ± SD	Control Gruop Mean ± SD	units
ALT	41.97±4.68	42.85±4.32	U/L
AST	153.75±13.25	153.43±14.32	U/L
ALP	135.6±13.6	141.4±15.6	U/L
A/G	0.4 ± 0.03	0.4 ±0.04	
BUN	6.19±0.55	6.21±0.64	mmol/L
WBC	12.13±1.25	12.24±1.58	10^{9}/L
RBC	9.98±0.41	10.21±0.51	10^{12}/L
HGB	164.52±1.53	165.32±2.08	g/L
PLT	839.14±40.61	838.59±42.72	10^{9}/L
HCT	47.2 ± 1.3	46.8± 1.3	%
MCV	54.19±4.15	53.46±3.66	fL
MCH	16.47±0.72	16.19±0.45	pg
MCHC	314.57±2.33	315.97±3.26	g/L

Notice: the data in the table is average calculated by five mice in each group. Healthy female mice i.v. injected with PEG/UCP were sacrificed at 2 weeks for blood collection. Serum biochemistry data including blood urea nitrogen (BUN) levels, albumin/globin ratios, and liver function markers: aspartate aminotransferase (AST), alkaline phosphatase (ALP), alanine aminotransferase (ALT), blood urea level (BUN), the ratio of albumin and globulin (A/G), red blood cells (RBC), white blood cells (WBC), mean corpuscular volume (MCV), hemoglobin (HGB), mean corpuscular haemoglobin (MCH), mean corpuscular hemoglobin concentration (MCHC), platelets (PLT), and hematocrit (HCT).